5th Joint International Symposium on Deformation Monitoring (JISDM), 20-22 June 2022, Valencia, Spain
DOI: http://doi.org/10.4995/JISDM2022.2022.13902

Monitoring Gravitational Deformations of the Wettzell 20 m Radio Telescope's Main Reflector Using a Leica RTC360

Agnes Weinhuber[1], Alexander Neidhardt[2], Christoph Holst[1]

[1] Technical University of Munich, School of Engineering and Design, Chair of Engineering Geodesy, Arcisstr. 21, 80333 Munich, Germany, (a.weinhuber@tum.de; christoph.holst@tum.de)
[2] Research Facility Satellite Geodesy, Technical University of Munich, Geodetic Observatory Wettzell, Sackenrieder Strasse 25, 93444 Bad Kötzting, Germany, (alexander.neidhardt@tum.de)

Key words: *laser scanning; deformation analysis; in situ calibration; VLBI; radio telescope; alignment*

ABSTRACT

Quasars are nowadays the basis to determine the world's absolute orientation in space by radio interferometry (VLBI). The global network of baselines measured by the used radio telescopes, which vary greatly in size, is subject to various influences that have an impact on the International Terrestrial Reference Frame. Among others, those influences are imperfections of individual panels of the dishes, a possible elevation dependent deformation of the whole dish and a shift of the reference point due to gravitational influences. In this study, we monitor the elevation dependent deformation of the main reflector of the 20 m radio telescope of the Geodetic Observatory Wettzell by a Leica RTC360 laser scanner. For this task, we mount the terrestrial laser scanner overhead near the subreflector to capture the surface of the moving dish at each elevation angle. This study focusses on 1) introducing further redundancy in the measurement and processing strategy to gain a reliable and accurate result even the used scanner is a no high-end one. This furthermore leads to 2) investigations whether there are differences in the results between in related work used high-end scanners and the RTC360 and thus 3) whether the RTC360 proves to be capable to detect deformations at a radio telescope's main reflector. Using these three foci, we show that deformations in the main reflector between elevations can be reliably determined areal and in focal length by redundant measurements with the RTC360. It is also shown that the results are less sensitive to axis errors compared to those obtained with high-end scanners. However, the compensations also show that the application scanner has certain systematics, which must be investigated in further steps.

I. INTRODUCTION

Globally distributed radio telescopes are used for the determination of the earth's absolute orientation in space, the linkage of different reference frames and also the establishment of the International Terrestrial Reference Frame (ITRF) (Nothnagel *et al.*, 2017). For the realization, radio telescopes – distribute all around the globe – record the radio signals emitted from quasars. By correlating the received signals of different radio telescopes, runtime differences in the signal and therefore differences in the distance between these telescopes and the quasars can be determined. Using multiple of dose measurements, a global network of baselines with uncertainties of 5 mm to 15 mm depending on the distance between the ground stations can be formed (Nothnagel *et al.*, 2004). This procedure is called very long baseline interferometry (VLBI). The positions of the radio telescopes, which are integrated into the local reference networks, can thus be determined with high precision of 1 - 4 mm (Nothnagel *et al.*, 2004).

In order to enable a highly accurate determination of the individual positions and guarantee a precise realization and maintenance of the global reference system, high accuracy requirements are correspondingly placed on the so-called local-ties. Therefore, all external circumstances, which may affect the reflectors of the radio telescopes, have to be taken into account. VLBI data already show different correction models. Nevertheless, but also not yet completely investigated and thus still unconsidered influences can, if they are uncovered and their magnitude made nameable, possibly lead to an improvement and support of the VLBI measurements (Nothnagel *et al.*, 2019). For example, Lösler *et al.* (2010) considered the effects of the ambient temperature on a possible change of position (2D) of the reference point of the radio telescope.

Laser scanning, which has come to the fore in recent years, allows radio telescope's geometries to be determined precisely and areal over their antenna surface. This now makes it possible, among other things, to detect possible imperfections of the entire reflector or of the individual panels (Holst *et al.*, 2015). Also, a determination of deformations of the telescope due to its own weight by approaching different elevation angles is and a possible influence on the reference point can be possible (Holst *et al.*, 2019). Due to the fact that laser scanning is becoming more and more popular and is used in many different application

fields, manufacturers are also producing laser scanners for mainstream consumers without any geodetic background and with lower requirements regarding accuracy and individual measurement procedures (*e.g.*, scanning in two faces, scanning only individual sections). As an example, the Leica RTC360 was built regarding this background.

This paper investigates how far measurements of the RTC360 for monitoring the radio telescope differ from comparable measurements with a high-end scanner. The recognizable differences and conspicuities in the course of the deformation analysis of the main reflector are highlighted. Furthermore, it is investigated whether this scanner is also suitable to detect the deformations at the telescope. Additionally, because a none high-end instrument is used, the measurements in this study are performed with higher redundancy to obtain reliable and accurate results.

After a short introduction of the monitoring procedures of radio telescopes in related work, technical data of the radio telescope in Wettzell and the used scanner are given and the chosen measuring procedure is described. In the main part the realization of the monitoring including the processing of the data and the deformation analysis is explained. Subsequently, the obtained results are evaluated regarding the deformation analysis and the used scanner.

II. Related Work

Laser scanning measurements enable a high quantity of points to be measured, which reflect the scanned object areal and with high precision. Thus, it is also possible to investigate deformations of objects in their entire surface. However, it is known from several investigations that a strict deformation analysis between individual points is not possible, since the recorded points are random points and not discrete points (Wunderlich *et al.*, 2019).

Several approaches have been developed to determine deformations between point clouds with high accuracy. One of them is the M3C2 algorithm, with which point clouds of different epochs, here the different elevations, can be compared to each other. The algorithm estimates planes and plane normals for so-called core points in suitably selected diameters in order to compare distances between these and the second point cloud (Lague *et al.*, 2013). However, this algorithm does not work optimally for detecting deformations of radio telescopes, even if the curvature of the main reflector is not steep. The required accuracies with which a deformation can be determined, however, cannot be achieved.

Since the design of a radio telescope is always a mathematically defined geometry, approaches are being developed which take the main reflector's shape into account and thus contribute to a successful deformation analysis. Using a CAD model describing the shape and comparing all elevations with this model turns out not to be useful. In a Cloud to Mesh comparison (C2M) the shortest distance of each point of the point cloud to the triangular surfaces is calculated. The algorithm is therefore suitable for objects that are as flat as possible (Lague *et al.*, 2013; Holst *et al.*, 2017). If a deformation is present, this will be detected, but due to the calculation of the point distance in a given direction, false assignments can occur, especially in the edge region of the reflector.

The mathematical description of a main reflector is thereby a mathematical rotational paraboloid defined by its focal length (Schlüter *et al.*, 2007). To gain a new approach for areal and meaningful deformation analysis for radio telescopes, Holst *et al.* (2012) develops a method where for each point cloud an estimation of a paraboloid is performed. By estimating the parameters of the reflector at each individual scanned state, the different elevation angles, the parameters for the focal length of the telescope are also estimated. The variation of the estimated focal lengths can therefore provide information about a deformation to the different elevation angles (Holst *et al.*, 2012). Previous work and analyses with 3D TLS data related to the observed radio telescope, deformations of the telescope can be detected by this method (Holst *et al.*, 2017; Holst *et al.* 2015).

III. Realization of the Monitoring

A. *Measurement Object*

The 20 m radio telescope at the Wettzell geodetic observatory, operated for almost 40 years now by the Federal Agency for Cartography and Geodesy (BKG) and the Satellite Geodesy Research Facility (FESG) of the Technical University of Munich, makes a decisive contribution to the realization and maintenance of the global reference system (Schlüter *et al.*, 2007). This radio telescope is a Cassegrain arrangement with main reflector and subreflector (BKG, 2022). The main reflector to be investigated can be described by a mathematical rotational paraboloid with a focal length of 9 m (Schlüter *et al.*, 2007). Here, possible influences of gravity due to the different elevation angles on the reflector are to be detected and determined.

B. *Measuring Procedure*

To cover the entire main reflector at the selected elevations in fine gradation of 5°, 10°, 20°, 30°, 40°, 50°, 60°, 70°, 80°, 90°, the scanner is mounted in the radio telescope (Figure 1). Thus, it can move with the dish at increasing elevations and there will be nearly no uncovered scan area. For the realization, the scanner was attached to one of the struts in the telescope with a mounting specially made for this radio telescope. Measuring in an inclined position is possible with the RTC360, but Leica Geosystems only recommends angles of up to 15° here (Leica, 2018). Accordingly, the mount allows the scanner to swing along to return to a vertical

upside-down orientation as the radio telescope moves to the next elevation step (Figure 2). The mount consists of an element with a magnetic brake in order to fix the laser scanner, which is oriented according to gravity, for the respective scan. This shall prevent the scanner from oscillating due to its own motion caused by the rotation of the scanner. To ensure the best possible view of the main reflector at each elevation angle, the scanner was therefore attached to one of the upper struts. It is also necessary to mount it as close as possible to the subreflector in order to minimize shadowing effects by the feed horn in the main reflector.

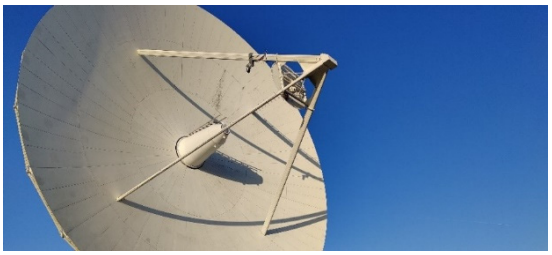

Figure 1. Mounting of the RTC360 in the 20 m Radio Telescope Wettzell.

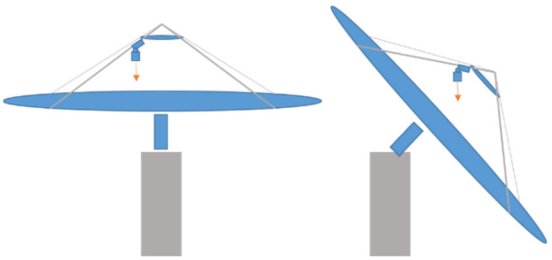

Figure 2. Mounting of the Laser Scanner and Measurement Principle in Different Elevation Angles (without scale)

In order to obtain redundant data for each selected elevation angle, the main reflector was scanned with a resolution of 3 mm at 10 m for each elevation angle when the radio telescope was raised to the upper elevations and it was also scanned when it lowered again. In the further writing, the differentiation between the increasing elevations (5° to 90°) and the decreasing (90° back to 5°) will be made by first and second measurement series. This results in two redundant scans for each of the elevation angle.

C. *Data Pre-Processing*

Calculating with high resolution point clouds requires an efficient data pre-processing. This pre-processing can be divided into several individual steps. When examining the radio telescope for deformations, the focus is on the main reflector. Therefore, this part must be extracted from the point cloud. For this purpose, all points outside the telescope are removed in a first step. Then, the components inside the telescope that do not belong to the parabolic main reflector, namely the sub-reflector, the feed and the struts, have to be removed (Figure 3). In a further step, outliers which often occur at edges or object boundaries during laser scanning are detected and removed manually (Figure 3). The outliers can be easily segmented by their intensity value, which is clearly different from the intensity values of the valid points on the telescope surface. The selected threshold value is thereby clearly defined that it can be applied to all point clouds and does not need to be adjusted.

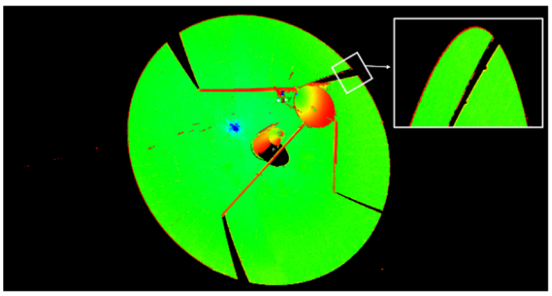

Figure 3. Point Clouds with Outliers. Detailed Cut-Out Shows the Higher Intensities in the Edge Area, Which Can Be Eliminated Via an Intensity Filter.

After removing the clearly detectable outlier points, there are still glancing points occurring between the single panels of the reflector, which are difficult to remove manually due to the curved shape (Figure 4). To remove them semi-automatically, the filter algorithm “Hidden Point Removal” in CloudCompare can be used. This filter is filtering all the points that lie in the background of the object from the current point of view (Katz *et al.*, 2007). By slightly tilting the point cloud and change the viewpoints, the glancing points between the panels and all close outlier points to the back of the reflector can be removed.

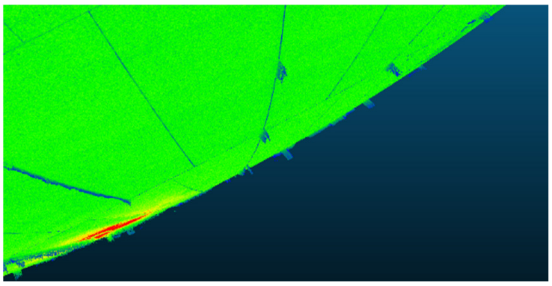

Figure 4. Back Side of a Scan Before Filtering with Hidden Point Removal, Outlier Between Panels.

To reduce the calculation time and the memory usage, the point clouds are also to be subsampled. Considering the further calculation steps to fit a concrete shape into the point clouds, a homogeneous point density in the point clouds of the main reflector are required. Only with an equal distribution an accurate parameter estimation is ensured (Holst *et al.*, 2017). The point clouds in this paper are subsampled to 1 cm point to point spacing. Therefore, the spatial subsampling tool of CloudCompare is used (CloudCompare, 2015).

D. *Data Processing – Shape Estimation*

In order to detect a possible deformation of the main reflector within the measured data, it must be taken into account for the further steps, that the reflectors

position changes in relation to the scanner due to the different elevation angles and the self-adjustment of the scanner in vertical direction.

The main reflector of the radio telescope in Wettzell consists of 3 rows of concentrically arranged panels, which together form the shape of a rotational paraboloid (Schlüter *et al.*, 2007). This allows the recorded measurement data to be parameterized with a functional model of a rotational paraboloid. In related work on deformation analysis of radio telescopes (Holst *et al.* 2018), it is outlined that the rotational paraboloid can be described in terms of focal length, for example as follows, if the axis of rotation equals the Z-axis of the [X, Y, Z] coordinate system (Eq. 1):

$$\frac{X_i^2 + Y_i^2}{4 \cdot f} - Z_i = 0 \tag{1}$$

where i = point cloud of i = 1, …, n sampling points
f = focal length

However, since the coordinates [x, y, z] of the point clouds are located in the scanner intrinsic coordinate system the paraboloid must be transformed by a three-dimensional Helmert transformation using two rotations and three translations (Niemeier, 2008) (Eq. 2):

$$\begin{bmatrix} X_i \\ Y_i \\ Z_i \end{bmatrix} = R_y(\phi_y) \cdot R_x(\phi_x) \cdot \begin{bmatrix} x_i \\ y_i \\ z_i \end{bmatrix} + \begin{bmatrix} X_t \\ Y_t \\ Z_t \end{bmatrix} \tag{2}$$

Accordingly, a rotational paraboloid can be described by 6 parameters in any position and orientation, here in the local scanner coordinate system, by: three translations in X, Y and Z direction, two rotations around x and y and the focal length f (Holst, 2017) (Eq. 3):

$$p = [X_t, Y_t, Z_t, \phi_x, \phi_y, f]^T \tag{3}$$

For the estimation of the parameters of the rotational paraboloid in the local scanner system, the measured coordinates in their original polar coordinates$[d, \varphi, \theta]$ must be integrated into the paraboloid model (Eq. 4):

$$\begin{bmatrix} x_i \\ y_i \\ z_i \end{bmatrix} = \begin{bmatrix} d_i \cdot \sin\ \varphi_i \cdot \cos\ \theta_i \\ d_i \cdot \sin\ \varphi_i \cdot \sin\ \theta_i \\ d_i \cdot \cos\ \varphi_i \end{bmatrix} \tag{4}$$

For this purpose, the coordinates have to be recalculated from the received Cartesian coordinates to their origin measured polar coordinates and for the further steps recalculated to the Cartesian coordinates again to then transform them into the coordinates of the paraboloid.

For the respective accuracies of the distances and angle measurements for the stochastic model Σ_{ll}, the manufacturer's specifications are used for the angel measurements φ and θ: $\sigma_{\varphi,\theta} = 5.6$ mgon (Leica, 2018) and for the range accuracy, σ_d is set to 1.5 mm for the stochastic model.

The parameters are calculated using the general case of adjustment (Gauß-Helmert-Model): the residuals $\hat{v}$ which represent the errors between the observations l and the adjusted observations $\hat{l}$ are reduced to a minimum (Mikhail and Ackermann, 1976): $v^T \Sigma_{ll}^{-1} v$.

To indicate possible deformations in the main reflector, the estimated paraboloid parameters $\hat{p}$ and the estimated residuals $\hat{v}$ are used. By using the residuals, information about the deformation of the reflector can be obtained as well as, for further research, systematic errors of the scanner can be detected (Holst *et al.*, 2018). This statement is based on the fact that the surface accuracy of the main reflector of the radio telescope is given as 0.35 mm rms (BKG, 2022) which is better than the scans.

E. *Deformation Analysis – Focal Length*

To get information about the deformation of the radio telescope, the estimated parameters can be examined. In Table 1, the estimated values for each elevation step of the first measurement series are considered. As described before, the shape of a rotational paraboloid is solely related to the size of the focal length f. It is prominent that the standard deviation of the focal length is estimated with $\sigma_f[mm] = 0.017$ for all elevation angles. This is too optimistic, which may be due to the fact that spatial correlation between neighboring points is neglected yet (Holst *et al.*, 2012). To get a better impression of the different focal lengths to the different elevation steps, differences of the increasing elevation steps to elevation step 5° are also shown as Δf in the table. The maximum difference reaches -5.0 mm between elevation 5° and elevation 80°, which validates the assumption that gravity effects the radio telescope's geometry in its different elevation angles.

Over the increasing elevation steps, the focal length becomes noticeably larger. To show this change graphically, the focal lengths of both measurement series are plotted for each elevation step in Figure 5. In the first measurement series (blue), there are rather none-smooth steps in the course of the connecting line between the values of the individual focal lengths. The maximum difference in the focal lengths between the first and the second measurement series is 0.4 mm (Table 2). If those finding are due to systematic measurement errors, will be evaluated in a prospective study.

F. *Deformation Analysis – Residuals*

In addition to considering the focal length, the areal measurement of the main reflector provides yet another way to visualize the deformations and check the success of the adjustments. Related work shows that by estimating the residuals and plotting the errors

in the points between the individual scans and the respective estimated paraboloid, deformations can be detected (Holst *et al.*, 2017). For this purpose, the errors are represented as intensities in the XY position of the rotational paraboloid.

The shown residuals in the range of - 5 to + 5 mm in the single plots show hardly any optical visible differences between the continuous elevation steps (Figure 6), but if the two extrema – elevation step 5° and 90° – are compared (additionally with another suitable color bar), visible differences appear in the maxima of the residuals (Figure 7). There are less maxima in the single points in elevation step 90°, which can be due to the fact that in elevation 90° the main reflector lies like an upward opened bowl and thus the force of the gravitation affects all areas approximately equally.

If the residuals are not considered in their total effect, but in their local maxima in the main reflector, then, on the one hand, the individual panels are clearly discernible. In the middle of the three concentric circles, the higher residuals occur more in the center of the panels, at the edges they tend to go into the negative range. In the outer and inner circles, the behavior seems to be reversed. The residuals can therefore also provide information about local deformations (Holst *et al.*, 2017).

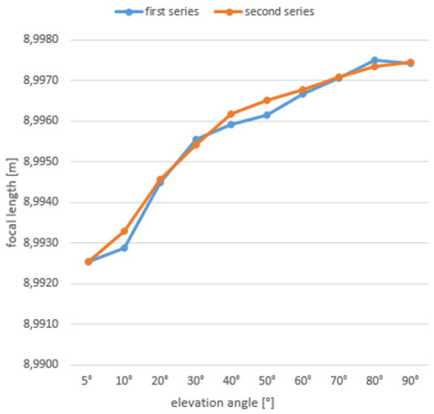

Figure 5. Focal Lengths f for all Elevation Levels in Both Measurement Series

Table 1. Estimated Parameters, First Series

p	Elevation angles [°]									
	5	10	20	30	40	50	60	70	80	90
X_t [m]	1.3589	0.9868	0.7603	0.1486	0.0179	0.1068	-0.3439	-0.5441	-0.8321	-1.2484
Y_t [m]	-1.1803	-1.5069	-1.6403	-1.8130	-1.8388	-1.8613	-1.8582	-1.8420	-1.7686	-1.5512
Z_t [m]	6.8021	6.7855	6.7352	6.6929	6.6498	6.6106	6.5815	6.5580	6.5432	6.5373
ϕ_x[gon]	-92.8248	-75.3197	-62.2525	-39.5589	-32.0068	-28.7366	-16.0541	-9.2608	-3.3473	-0.0241
ϕ_y[gon]	45.6064	70.0086	58.3387	58.0302	47.6971	35.26131	29.6200	20.3403	10.6671	0.0219
f [m]	8.9926	8.9929	8.9945	8.9956	8.9959	8.9962	8.9967	8.9971	8.9975	8.9974
σ_f $[mm]$	0.017	0.017	0.017	0.017	0.017	0.017	0.017	0.017	0.017	0.017
Δf[mm]	-	-0.3	-1.9	-3.0	-3.4	-3.6	-4.1	-4.5	-5.0	-4.9

Table 2. Differences in f between First and Second Measurement Series

p	Elevation angles [°]									
	5	10	20	30	40	50	60	70	80	90
f_1 [m]	8.9926	8.9929	8.9945	8.9956	8.9959	8.9962	8.9967	8.9971	8.9975	8.9974
f_2 [m]	8.9926	8.9933	8.9946	8.9954	8.9962	8.9965	8.9968	8.9971	8.9973	8.9974
Δf_{2-1}[mm]	0	0.43	0.06	0.14	0.26	0.36	0.11	0.03	0.17	0.02

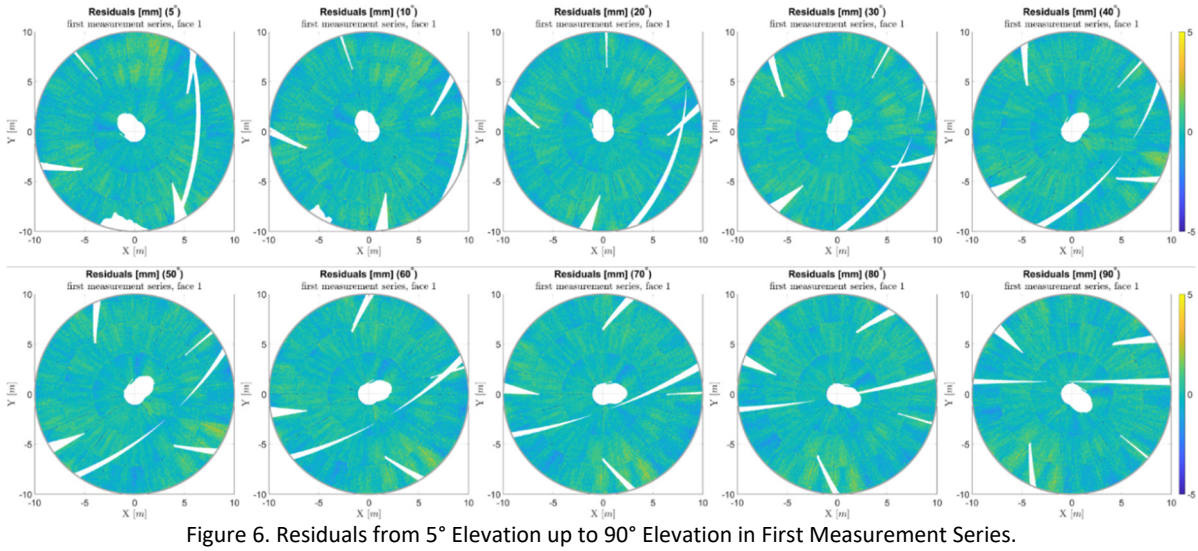

Figure 6. Residuals from 5° Elevation up to 90° Elevation in First Measurement Series.

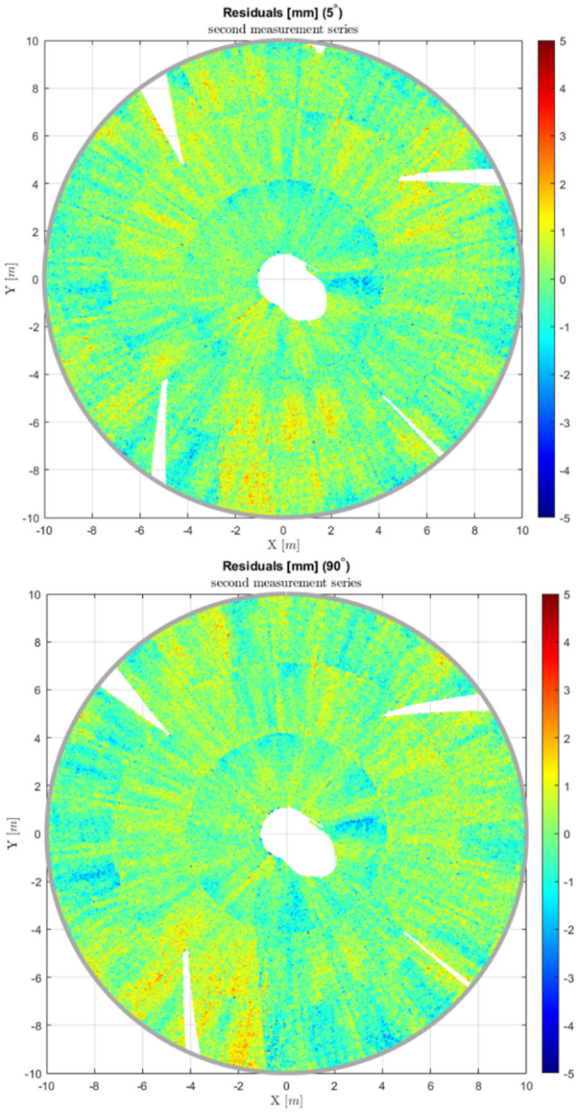

Figure 7. Residuals for the Elevations 5° and 90° in the Second Measurement Series.

Furthermore, a leap in the representation between positive and negative residuals is clearly visible, which indicates systematic deviations of the scanner due to its axis error (Figure 8). This systematic is to be expected, but it is interesting to note that the differences are much smaller than in the previous works (Holst *et al.*, 2018), which is to be investigated in further steps. As well, a purely optical comparison of the plots of the first and second measurement series does not show any recognizable differences between the two plots of the 90° elevation (not shown here). In elevation 5°, however, the positive maxima in the plot is more clearly recognizable.

When zooming in close to one of the plots, stripe-like patterns that converge from the upper edge of the main reflector to the center appear (Figure 8). This effect indicates that the holder was possibly not quite stable during the scan and the scanner could oscillate. Furthermore, the change of sign in the residuals (around X=-1m) clearly indicates systematic calibration errors of the scanner (compare to Holst *et al.*, 2017).

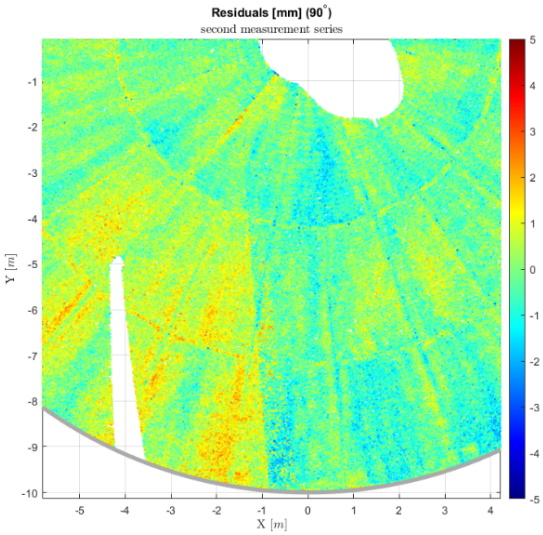

Figure 8. Leap Due to Systematic Deviations of the Scanner Axis Errors.

IV. Evaluation of the Results

A. *Deformation Analysis*

In this study, it was demonstrated that by means of the areal measurements and the high resolution of terrestrial laser scanning, conclusions can be made about the deformations of the main reflector of a radio telescope. By the calculated residuals between the single scans and the equivalent estimated rotational paraboloid, local deformations at the panels can be detected (Holst *et al.*, 2017) and highlighted by meaningful values in further investigations as well as in related work. Deformations of the entire reflector can also be highlighted via a holistic view of the plotted residuals. With further scans of the main reflector in a first and second cycle, scanner-internal effects can be eliminated by co-estimating calibration parameters in an in-situ calibration (Holst *et al.*, 2015). Related work also shows that by estimating calibration parameters, there is the possibility of a clear separation between influences of the scanner and the actual deformations due to the effect of gravity on the reflector at different elevation angles (Holst and Kuhlmann, 2016).

Furthermore, this paper shows that by estimating the parameters for the individual scans, unambiguous statements can be made about the deformations depending on the elevation when the parameters for the focal lengths are compared. A rotational paraboloid flattens with increasing focal length. If this is transferred to the data obtained, the effect can be seen. If the reflector is in the elevation step 90°, the gravitation has the same effect on the whole dish due to the position, the focal length is larger and the paraboloid is therefore flatter. If the dish is lowered towards the ground, the focal lengths become steadily smaller, which indicates that the upper edge of the dish presses down more strongly and a deformation due to gravity is confirmed.

Although the differences in the focal lengths between the two series of measurements shown in Figure 5 only

reach values in the sub-millimeter range, these must be considered in further investigations. An estimation of the parameters in the adjustment in ascending as well as in descending direction for the first and second measurement series, which would result four values for the focal length, could lead to more insights. In this study, both series were calculated with initial values for the elevation of 5° in ascending elevation direction.

B. *RTC360 Investigations*

It has been shown that the RTC360 is suitable for upside-down measurements and detecting deformations in the radio telescope's shape. The systematic axis errors that are clearly visible in previous work occurring with scanners not explicitly designed for upside-down measurement are also present in the measurements with the RTC360 but are far less noticeable. The range of deviations that can occur in a single panel are almost as large as the leap due to the axis error. No reason has been found yet why the RTC360 results seem less prone to error.

To smooth the small visible transition due to the axis errors and get more insights about the scanner itself, the RTC360 can be brought in a second manually rotated position to measure cycle 2. By that, an estimation of the calibration parameters can be made (Holst *et al.*, 2017).

Another systematic is also revealed: It seemed like the local coordinate system of the RTC360 changes between the individual scans. This effect can be clearly seen in the rotation of the main reflector in the plots of the residuals (Figure 6). To check the effect, all scans of the first measurement series and second measurement series were displayed together (Figure 9). Without this effect, series 1 and 2 should be congruent. However, a fanning out and a rotation like a twisting to each other can be seen. How the coordinate system is moving and if this systematic degrades the deformation analysis, need to be investigated and proven in further steps.

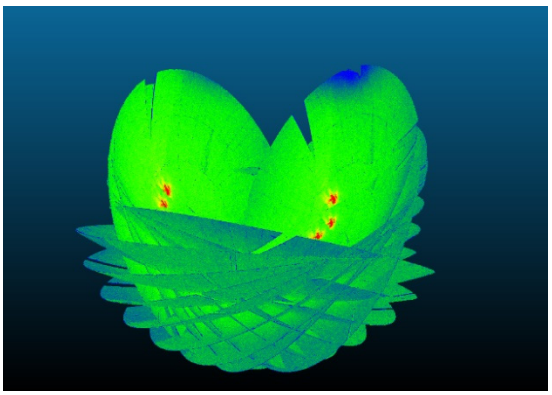

Figure 9. Systematic of RTC360 in Ongoing Scans (left: First Measurement Series; right: Second Measurement Series).

Here, a difficulty is that the exact internal pre-processing steps of a laser scanner remain hidden from the user and are not communicated by the manufacturer or only to a limited extent, what leads to the designation of a black box system (Woschitz and Heister, 2017). Because the RTC360, in order to facilitate operation for the general and non-professional use, has a strongly predefined and limited selection of operating settings, which manipulate the data on the run (*e.g.*, the Doule Scan function), the internal processing steps behind it make it even more of a black box system. Thus, it is not only difficult to obtain further information about raw data but especially about the integrated sensors data like the IMU. To get an idea about the behavior of the scanner, further studies have to be done to investigate the rotations in Figure 9.

V. Conclusion

By the approved method to estimate a rotation paraboloid for each elevation by means of an adjustment into each scan, statements about elevation dependent deformation of the main reflector of the 20 m radio telescope of the Geodetic Observatory Wettzell can be made. The results of the adjustment show that the application scanner has some peculiarities and systematics compared to the high-end scanners used in previous works, which have to be investigated in further steps. Nevertheless, the results of the RTC360 can be assumed to be valid. This is supported by comparisons of the estimated parameters of the rotational paraboloid at each elevation angle between the redundant measurements in ascending order and again in descending order.

References

BKG, (2022). Bundesamt für Kartographie und Geodäsie. Avalaible in: http://www.bkg.bund.de/DE/Observatorium-Wettzell/, last accessed January 28.

Cloudcompare, (2015). Girardeau-Montaut, D.. Available in: http://www.danielgm.net/cc/, last accessed January 27, 2022.

Holst, C., P. Zeimetz, A. Nothnagel, W. Schauerte, and H. Kuhlmann, (2012). Estimation of focal length variations of a 100-m radio telescope's main reflector by laser scanner measurements. In: *Journal of Surveying Engineering*, 138(3), pp 126-135.

Holst, C., A. Nothnagel, M. Blome, P. Becker, M. Eichborn, and H. Kuhlmann, (2015). Improved area-based deformation analysis of a radio telescope's main reflector based on terrestrial laser scanning. In: *Journal of Applied Geodesy*, 9(1), pp 1-14.

Holst, C., and H. Kuhlmann, (2016). Challenges and present fields of action at laser scanner based deformation analyses. In: *Journal of Applied Geodesy*, 10(1), pp 17-25.

Holst, C., B. Schmitz, A. Schraven, and H. Kuhlmann, (2017). Eignen sich in Standardsoftware implementierte Punktwolkenvergleiche zur flächenhaften Deformationsanalyse von Bauwerken? Eine Fallstudie anhand von Laserscans einer Holzplatte und einer Staumauer. In: *Zeitschrift für Vermessungswesen* (zfv), 2.

Holst, C., D. Schunck, A. Nothnagel, R. Haas, L. Wennerbäck, H. Olofsson, R. Hammargren, and H. Kuhlmann, (2017).

Terrestrial laser scanner two-face measurements for analyzing the elevation-dependent deformation of the onsala space observatory 20-m radio telescope's main reflector in a bundle adjustment. In: *Sensors*, 17(8), 1833.

Holst, C., T. Medić, and H. Kuhlmann, (2018). Dealing with systematic laser scanner errors due to misalignment at area-based deformation analyses. In: *Journal of Applied Geodesy*, 12(2), pp 169-185.

Holst, C., A. Nothnagel, R. Haas, and H. Kuhlmann, (2019). Investigating the gravitational stability of a radio telescope's reference point using a terrestrial laser scanner: Case study at the Onsala Space Observatory 20-m radio telescope. In: *ISPRS Journal of Photogrammetry and Remote Sensing*, 149, pp 67-76.

Katz, S., A. Tal, and R. Basri, (2007). Direct visibility of point sets. In: *ACM SIGGRAPH 2007 papers*, pp. 24-es.

Lague, D., N. Brodu, and J. Leroux, (2013). Accurate 3D comparison of complex topography with terrestrial laser scanner: Application to the Rangitikei canyon (NZ). In: *ISPRS Journal of Photogrammetry and Remote Sensing*, 82, pp 10-26.

Leica Geosystems AG, (2018). RTC360. Available in: https://leica-geosystems.com/, last accessed January 28.

Lösler, M., C. Eschelbach, A. Schenk, and A. Neidhardt, (2010). Permanentüberwachung des 20 m VLBI-Radioteleskops an der Fundamentalstation in Wettzell. In: *Zeitschrift für Vermessungswesen* (zfv), 135(1), pp 40-48.

Mikhail, E., and F. Ackermann, (1976). *Observations and Least Squares* (1976). In: Dun-Donelly, New York, NY, pp 497.

Niemeier, W., (2008). *Ausgleichungsrechnung. Statistische Auswertemethoden*. Berlin: de Gruyter, 2. Auflage.

Nothnagel, A., W. Schlüter, and H. Seeger, (2004). Die geodätische VLBI in Deutschland. In: *Zeitschrift für Vermessungswesen* (zfv), 129, pp 219-226.

Nothnagel, A., T. Artz, D. Behrend, and Z. Malkin, (2017). International VLBI service for geodesy and astrometry. In: *Journal of Geodesy*, 91(7), pp 711-721.

Nothnagel, A., C. Holst, and R. Haas, (2019). A VLBI delay model for gravitational deformations of the Onsala 20 m radio telescope and the impact on its global coordinates. *Journal of Geodesy*, 93(10), pp 2019-2036.

Schlüter, W., N. Brandl, R. Dassing, H. Hase, T. Klügel, R. Kilger, P. Lauber, A. Neidhardt, C. Plötz, S. Riepl, and U. Schreiber, (2007). Fundamentalstation Wettzell-ein geodätisches Observatorium. In: *Zeitschrift für Vermessungswesen* (zfv), 132(3), pp 158-167.

Woschitz, H., and H. Heister, (2017). *Überprüfung und Kalibrierung der Messmittel in der Geodäsie*. In: Ingenieurgeodäsie, Springer Spektrum, Berlin, Heidelberg, pp 403-461.

Wunderlich, T., L. Raffl, and W. Wiedemann, (2019). *Wiedererkennung–zwei Lösungen für die strenge Deformationsanalyse flächenhafter Beobachtungen der Ingenieurgeodäsie*. In: Hanke K, Weinold T (eds), 20, pp 264-273.